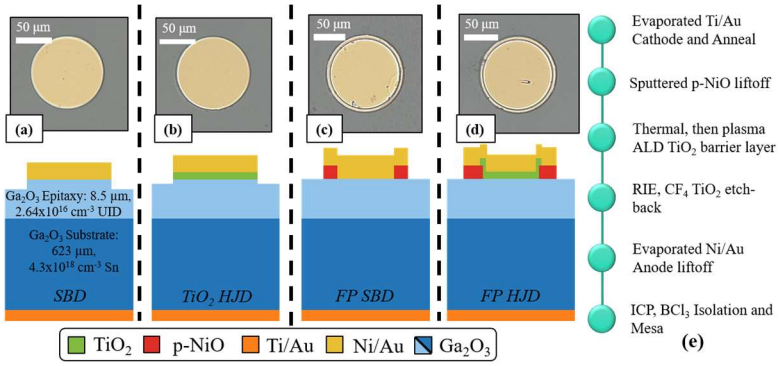

Fig. 1 Optical microscope and cross section graphic depicting each device type: (a) SBD (b) TiO_2 HJD (c) GR SBD (d) GR HJD; and (e) an outline of the fabrication process flow.

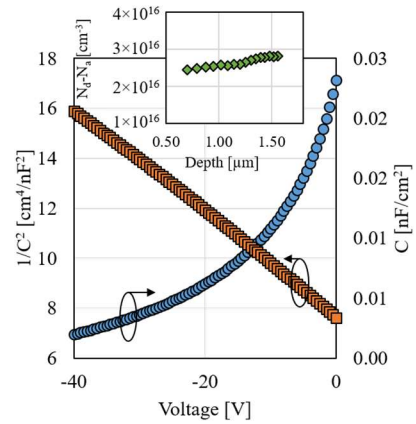

Fig. 2 C-V measurements of an SBD device with extracted carrier concentration vs. depth.

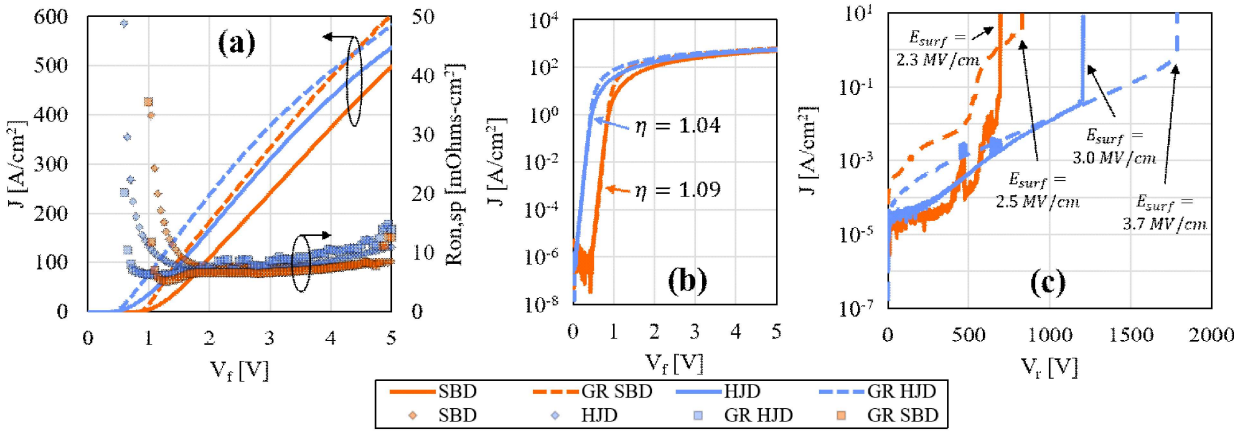

Fig. 3 (a) Forward J-V response of each device on a linear scale with differentially extracted $R_{on,sp}$. (b) Forward J-V response on a logarithmic scale with extracted ideality factors. (c) Reverse bias J-V response and breakdown, with surface electric field at breakdown calculated from C-V derived doping and manufacturer specifications.

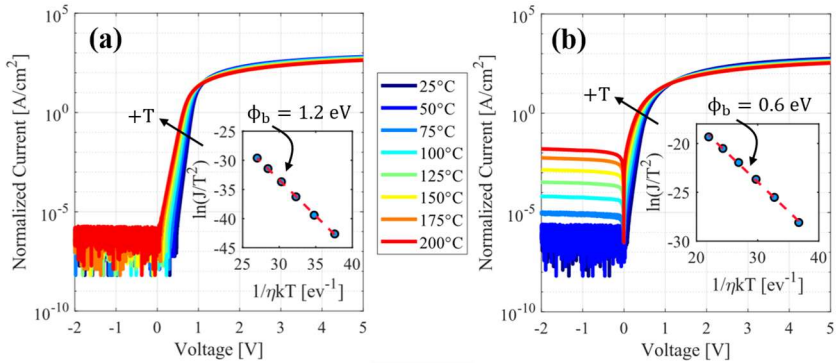

Fig. 4 Temperature dependent J-V response of a representative (a) SBD device and (b) TiO_2 HJD device. The inset shows Richardson plots used for extracting each junction barrier height according to the classical thermionic emission model.

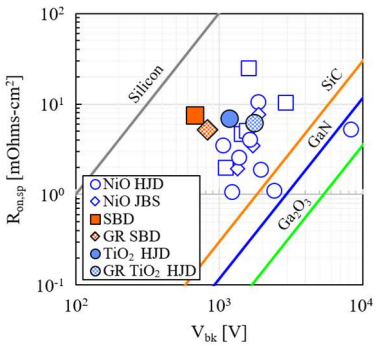

Fig. 5 The devices from this work (filled points) compared with literature (empty points) using BFOM = $V_{bk}^2/R_{on,sp}$.